A Monolithically Integrated Two-Section Laser for Wideband and Frequency-Tunable Photonic Microwave Generation

Cai, Qiang; Zhang, Yunshan; Zheng, Jilin; Zhang, Yamei; Li, Pu; Shore, K. Alan; Wang, Yuncai

Journal of Lightwave Technology

DOI:
10.1109/JLT.2022.3216452

Published: 15/01/2023

Peer reviewed version

This article has been accepted for publication in IEEE/OSA Journal of Lightwave Technology. This is the author's version which has not been fully edited and content may change prior to final publication. Citation information: DOI 10.1109/JLT.2022.3216452

A Monolithically Integrated Two-Section Laser for Wideband and Frequency-Tunable Photonic Microwave Generation

Qiang Cai, Yunshan Zhang, Jilin Zheng, Yamei Zhang, *Member, IEEE*, Pu Li, K. Alan Shore, *Senior Member, IEEE,* and Yuncai Wang

***Abstract*—A monolithically integrated two-section laser is presented for wideband and frequency-tunable photonic microwave generation. The laser consists of two back-to-back DFB sections forming a mutually coupled structure. By properly adjusting the bias currents of two sections, the laser can stably work at the state of period-one oscillation over a wide range of frequency detuning. Based on this, continuous and linear tuning of photonic microwave signals can be achieved. Experimental results confirm that a large tunable range from 12.45 to 80.30 GHz can be realized using this laser.**

***Index Terms*—Photonic microwave generation, monolithic integrated circuits, mutually coupled laser, period-one oscillation.**

I. Introduction

Microwave oscillators are crucial components for wireless and mobile communication systems. With the increasing capacity demand of high-speed interactive multimedia services, there is a pressing need for microwave signal generation systems that can operate at high frequencies and with an ultrawide bandwidth [1], [2]. Conventional electronic microwave oscillators usually have a low frequency at the level of GHz. For higher frequencies, they experience rapid performance degradation due to the introduction of multiple stages of frequency doubling [3].

To overcome this issue, microwave signal generation using photonic approaches has attracted much research interest due to its advantages such as high bandwidth, low power consumption and high reliability [4]. Various photonic schemes for microwave generation have been studied, but they are mainly based on six different mechanisms or devices: direct modulation [5], [6], external modulation [7], [8], optoelectronic oscillators (OEOs) [9], [10], optical heterodyne [11]-[13], dual-mode lasers [14]-[17], and period-one (P1) nonlinear dynamics in semiconductor lasers [18]-[30]. For the schemes based on direct and external modulation, their generated microwave signals usually have a limited frequency by the relaxation oscillation of the used semiconductor laser or the modulator bandwidth [5]. OEO-based schemes can improve this problem, but they usually are at the cost of increasing the system complexity [9]. The optical-heterodyne-based approaches detecting two independent lasers with different wavelengths can easily produce high-frequency microwave signals, but their phase noise is very high because the two lasers commonly are not phase correlated [12]. Using a dual-mode laser can emit simultaneously two lasing modes with locked phase so that their generated microwave signals process a high spectral purity. However, this approach using the dual-mode lasers has a poor tuning ability due to the fixed frequency spacing between the two lasing modes [14].

Compared with these techniques mentioned above, the P1-based method offers some unique advantages for photonic microwave generation: (i) this method is an all optical scheme with a simple configuration and thus not suffering from limited electronic bandwidths [22]. (ii) The microwave frequency generated by P1 oscillation can be broadly tuned from a few to tens of GHz by simply adjusting the strength and detuning-

This work was supported in part by the National Natural Science Foundation of China under Grants (62175177, 61927811, 61731014 and U19A2076); in part by the Program for Guangdong Introducing Innovative and Entrepreneurial Teams; in part by the Natural Science Foundation of Shanxi Province under Grant (201901D211116; 201901D211077); in part by Sichuan Science and Technology Program (2022YFG0330). *(Corresponding author: Pu Li)*.

Q. Cai is with the Key Laboratory of Advanced Transducers and Intelligent Control System, Ministry of Education, Taiyuan University of Technology, Taiyuan 030024, China (email: caiqiang0414@163.com).

Y. S. Zhang is with the College of Electronic and Optical Engineering and the College of Microelectronics, Nanjing University of Posts and Telecommunications, Nanjing 210023, China (e-mail: yszhang@njupt.edu.cn).

J. L. Zheng is with the College of Communications Engineering, Army Engineering University of PLA, Nanjing 210007, China (e-mail: zhengjl@nju.edu.cn).

Y. M. Zhang is with the Key Laboratory of Radar Imaging and Microwave Photonics, Ministry of Education, Nanjing University of Aeronautics and Astronautics, Nanjing 210016, China (e-mail: zhang_ym@nuaa.edu.cn).

P. Li is with the Key Laboratory of Advanced Transducers and Intelligent Control System, Ministry of Education, Taiyuan University of Technology, Taiyuan 030024, China, and the Guangdong Provincial Key Laboratory of Photonics Information Technology, School of Information Engineering, Guangdong University of Technology, Guangzhou 510006, China (e-mail: lipu8603@126.com).

K. A. Shore is with the School of Electronic Engineering, Bangor University, Wales LL57 1UT, United Kingdom (e-mail: k.a.shore@bangor.ac.uk).

Y. C. Wang is with the Guangdong Provincial Key Laboratory of Photonics Information Technology, College of Information Engineering, Guangdong University of Technology, Guangzhou 510006, China (email: wangyc@gdut.edu.cn).

This article has been accepted for publication in IEEE/OSA Journal of Lightwave Technology. This is the author's version which has not been fully edited and content may change prior to final publication. Citation information: DOI 10.1109/JLT.2022.3216452

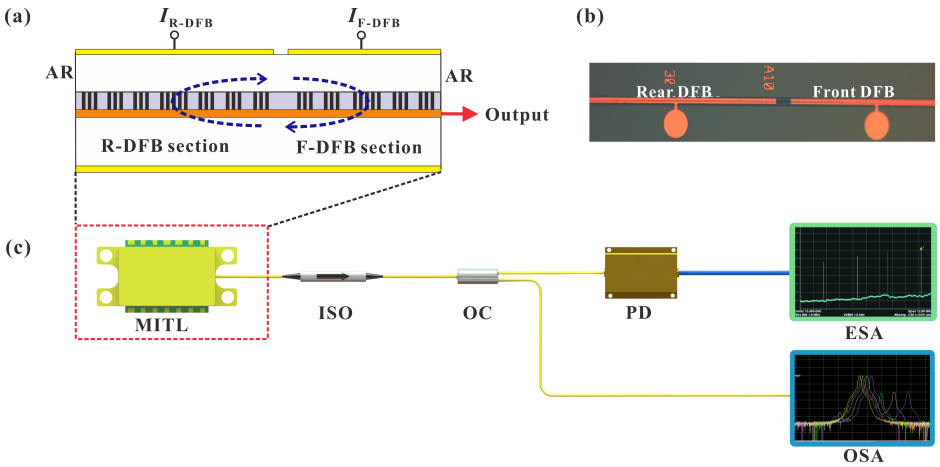

Fig. 1. (a) Schematic diagram of the MITL, (b) Photograph of the MITL, and (c) Experimental setup for generating and measuring the photonic microwave signals. MITL: monolithically integrated two-section laser; IOS: isolator; OC: 90:10 optical coupler; PD: photodetector; ESA: electric spectrum analyzer: OSA: optical spectrum analyzer.

frequency of the optical injection [23]-[26]. (iii) this technique has a single sideband (SSB) optical spectra structure and thus the associated microwave signals have the merit of low phase noise [27]. Although outstanding progresses the photonic microwave generation utilizing P1 nonlinear dynamics have been made, most of reported P1-based schemes are constructed using discrete optical devices and thus their whole systems are bulky and unstable.

In recent years, photonic integrated chips (PICs) show the potential for greatly reducing the system complexity and size of the P1-bassed microwave generation schemes [31]. Typically, there are two kind of integration schemes for P1 oscillation. One scheme is the optically feedback laser [32]. However, this scheme has a very low tuning ranges of only a few GHz being limited by the insufficient parameter space. The other scheme is the optically injected laser [33]. Compared with the optical feedback scheme, this optical injection scheme enables broadly tunable microwave generation. However, the PICs based on optical injection usually consist of three sections (two laser sections and one phase section) up to now. The efficient length of the phase section is very sensitive to temperature variations [34], [35]. This will significantly affect the stability of the associated time delay between the two DFB sections, so that the continuous tuning range is very difficult to be enhanced further.

To solve the problem of insufficient tuning-range confronted by the P1-based technique, we propose a monolithic integrated two-section laser (MITL) in this paper for photonic microwave generation [36]-[39]. In contrast with the aforementioned PICs with optical injection, our MITL is constructed of two back-to-back DFB sections with a mutually coupled geometry and its structure is largely simplified. Experimental results show that this MITL can output wideband and frequency-tunable microwave signals by adjusting the bias current of these two DFBs. Quantitatively, its operation frequency can be continuously tuned from 12.45 to 80.30 GHz, which corresponds to a tuning range of about 68 GHz. Moreover, it should be emphasized that the frequency of photonic microwave increases linearly (not nonlinearly like in Ref. [33]), when we enhance the bias current of the associated DFB section. This is another merit of our two-section laser over the existing PICs for photonic microwave generation.

II. Experimental Setup and Results

Figs. 1(a) and 1(b) show the schematic diagram and photograph of the MITL, respectively. The laser consists of a rear DFB (R-DFB) section of length 450 μm and a front DFB (F-DFB) section of length 350 μm, which are electrically isolated from each other. Both DFBs are monolithically integrated on an InGaAlAs multiple quantum well (MQW) material and grown on an indium-phosphide (InP) substrate in the epitaxial structure by a conventional two-stage metal organic chemical vapor deposition (MOCVD). The grating of R-DFB and F-DFB is made using the reconstruction-equivalent-chirp (REC) technique [40] and has an equivalent π phase shift to obtain a single longitudinal mode yield. Antireflection (AR) coatings with reflectivity of less than 1% are deposited on both facets. The two DFB sections are fabricated back-to-back with a mutually coupled structure, and they are driven by two independent currents labelled as $I_{R\text{-}DFB}$ and $I_{F\text{-}DFB}$ in Fig. 1(a). Finally, the generated photonic microwave signal comes out from the right side of the F-DFB section.

Fig. 1(c) illustrates the experimental setup for measuring the photonic microwave signal. The MITL is powered by two high accuracy current sources (ILX Lightwave LDX-3412), while its temperature is stabilized at 24.5°C with a thermoelectric controller (ILX Lightwave LDT-5412B). The photonic microwave output of the MITL passes through an isolator to prevent unwanted feedback disturbance and then is split into two parts by a 90:10 fiber coupler. One part (10%) is recorded by an optical spectrum analyzer (OSA, Yokogawa, AQ6370C), and the other part (90%) is detected by an electric spectrum analyzer (ESA, Rohde & Schwarz, FSW-50, 50 GHz bandwidth) after a high-speed photodetector (PD, Finisar, XPDV2120RA, 50 GHz bandwidth).

Before generating the microwave signal, we measure the optical spectra of the F-DFB section in the MITL. An ideal single mode

operation is required for P1-based photonic microwave generation. Fig. 2 shows the measured optical spectra of F-DFB under different bias currents $I_{\text{F-DFB}}$ when the current of R-DFB is unbiased (i.e., $I_{\text{R-DFB}}$ = 0 mA). From it, we can confirm that the F-DFB always has a very high side-mode-suppression-ratios (SMSRs) about 60 dB. This means that this F-DFB does not generate redundant frequency components induced by the possible interactions between the main mode and other side modes. At the same time, it also can be observed that the lasing wavelength moves to the longer side with a tuning efficiency of 0.0093 nm/mA, when the bias current increases. The origin of the red-shift for free-running F-DFB in Fig. 2 is from the refractive-index change of the active region induced by the increased bias current [41]. In a free-running laser, the refractive index $n(I)$ of the active region is linear with the bias current I and can be expressed as $n(I)= n_0+K_r (I- I_0)$. Note, n_0 is the refractive index when the injection current is I_0, while K_r is a scale coefficient. Then, the associated wavelength shift $\Delta\lambda$ can be calculated as follows:

$$\Delta\lambda=\frac{\Delta n}{n_0}\lambda_0 \tag{1}$$

Note, Δn is the effective refractive index change, and λ_0 is the lasering wavelength corresponding the bias current I_0.

We point that limited by the encapsulated package, the output of R-DFB cannot be directly measured, but it is expected that the R-DFB should also exhibit a single-mode oscillation when it works independently because it has the same grating structure as that of the F-DFB.

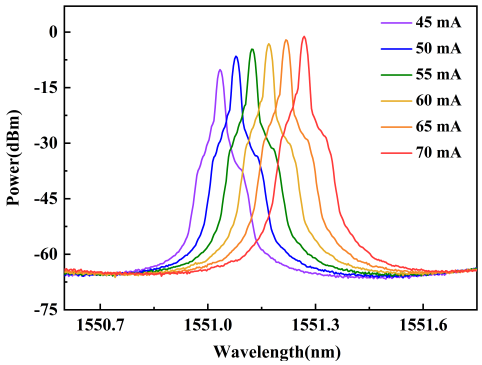

Fig. 2. Measured optical spectra of the free-running F-DFB. The bias current of $I_{\text{R-DFB}}$ is unbiased, and the current of $I_{\text{F-DFB}}$ is biased at 45 mA, 50 mA, 55 mA, 60 mA, 65 mA, and 70 mA, respectively.

Next, we consider photonic microwave generation. In the experiment, the bias current of the F-DFB is fixed at 60 mA, while the current injected into the R-DFB is adjusted in the range from 40 to 100 mA. Due to the temperature and carrier density variations, different frequency detuning between these two DFBs appears. Fig. 3 shows the associated optical spectra [left column] and the radio frequency (RF) spectra [right column] at different detuning frequencies. Fig. 3(a-i) depicts the measured optical spectrum when $I_{\text{R-DFB}}$ =40 mA and $I_{\text{F-DFB}}$ =60 mA. From it, we can see that the detuning frequency Δf can be ignored, so the R-DFB are locked by F-DFB and thus the lasing wavelength of F-DFB can be observed. This does not mean that both the free-running F-DFB and R-DFB have the same lasing wavelength at different bias currents. In fact, there is a frequency detuning between the F-DFB biased at 60 mA and R-DFB at 40 mA. Due to its low bias current, the R-DFB with low power is injection-locked by the F-DFB with a large power. In consequence, only the lasing wavelength of F-DFB is observed. Note, the lasing wavelength of F-DFB moves to the longer side compared with its free-running state at the same condition in Fig. 2. Different with the free-running F-DFB in Fig. 2, the F-DFB in Fig. 3 is optically injected by another laser (i.e., the R-DFB). In this case of optical injection, the red-shift of the F-DFB wavelength is induced by the cavity resonance shift [42]. Specifically, with the increase of the optical injection strength (the bias current of the R-DFB), the optical gain deficit of the F-DFB increases. Due to the anti-guidance effect, the refractive index increases and thus the cavity resonance shifts red. In addition, its flat RF spectrum without any prominent peaks [Fig. 3(a-ii)] further confirm that the MITL indeed operates at a stable continuous wave (CW) state.

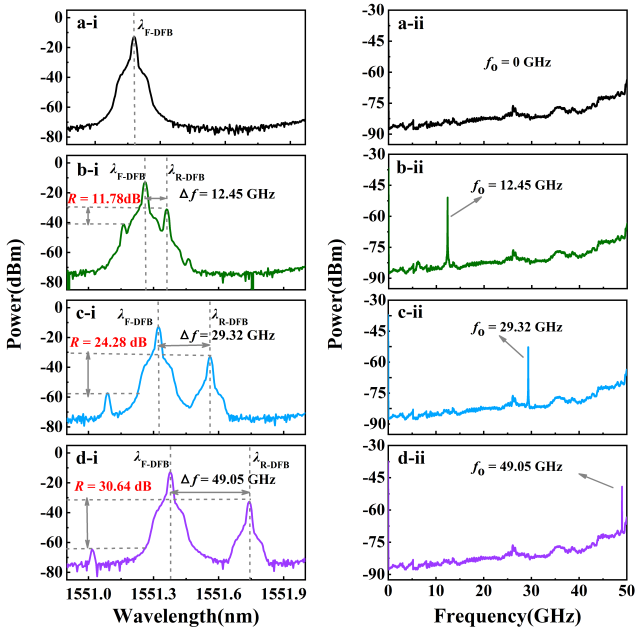

Fig. 3. Measured optical spectra (left) and RF spectra (right). The bias current of $I_{\text{F-DFB}}$ is fixed at 60 mA, and the current of $I_{\text{R-DFB}}$ is biased at (a) 40 mA, (b) 42.5 mA, (c) 55 mA, and (d) 71.6 mA, respectively.

When the bias current $I_{\text{R-DFB}}$ increases to 42.5 mA, the F-DFB is subjected to a relatively strong optical injection and a larger detuning frequency. Thus, the laser undergoes a Hopf-bifurcation to the state of P1 oscillation [43], as shown in Fig. 3(b). In this case, ones can find from Fig 3(b-i) that the optical spectrum is dominated by both the principal wavelength component of the F-DFB (labelled as $\lambda_{\text{F-DFB}}$) and the regenerated injection frequency of the R-DFB (labelled as $\lambda_{\text{R-DFB}}$). In consequence, the MITL operates at a single sideband (SSB) P1 oscillation, which is desirable for photonic microwave generation. Quantitatively, the P1 frequency f_o is measured to be 12.45 GHz, which equals the after-injection detuning frequency Δf between R-DFB and F-DFB [Fig. b(a-ii)].

Further increasing the bias current $I_{\text{R-DFB}}$, we can obtain a higher frequency of photonic microwave. For instance, when the bias current $I_{\text{R-DFB}}$ is increased to be 55 mA, the measured optical spectrum and RF spectrum are shown in Fig. 3(c). After calculation, the detuning frequency Δf between R-DFB and F-DFB is 29.32 GHz [Fig. 3(c-i)], and accordingly the MITL generates a

photonic microwave with a high frequency of 29.32 GHz [Fig. 3(c-ii)]. Limited by the measuring range of the available PD and ESA, the highest frequency 49.05 GHz of the generated photonic microwave is observed when $I_{R\text{-}DFB}$ is biased at 71.6 mA, as shown in Fig. 3(d).

We emphasize that in our method the microwave signal is generated by the period-one (P1) oscillation in the optically injected laser system, not optical heterodyne. Hence, there is a typical feature for P1 oscillation that under different operating conditions there are some side-bands in the optical spectra except for the principal oscillation [44]. In our experiment, the F-DFB and R-DFB are mutually injected each other and thus three different peaks in Figs. 3(b)-(d) appear as follows: (i) The two high peaks correspond to the principal oscillation $\lambda_{F\text{-}DFB}$ and injection frequency $\lambda_{R\text{-}DFB}$, respectively; (ii) The third peak represents another sideband. The frequency separation between the second sideband and principal oscillation $\lambda_{F\text{-}DFB}$ is the same as that between the principal oscillation $\lambda_{F\text{-}DFB}$ and injection frequency $\lambda_{R\text{-}DFB}$, indicating that the sideband is a harmonic signal of of the first sideband (i.e., injection frequency $\lambda_{R\text{-}DFB}$) due to the inherent nonlinearity of the optically injected lasers.

Furthermore, we point that all the measured RF signals are single-mode, as shown in Figs. 3(b-ii) to 3(d-ii). The physical mechanism behind the P1 oscillation can be viewed as the beating of two dominating wavelengths: one is regenerated from the optical injection while the other is emitted near the cavity resonance wavelength [43]. From the optical spectra in Figs. 3(b-i) to 3(d-i), we can determine that the two dominating wavelengths in our experiment is just $\lambda_{F\text{-}DFB}$ and $\lambda_{R\text{-}DFB}$. Therefore, only a single mode exists in the associated RF spectra in Figs. 3(b-ii) to 3(d-ii). In theory, the second harmonic induced by the second sideband and $\lambda_{R\text{-}DFB}$ could produce another microwave tone. However, the high sideband suppression ratio R at least higher than 10 dB [Figs. 3(b-i) to 3(d-i)]) make the possible second harmonic be so weak that it will be submerged in background noise in practice. Note, R is quantitatively defined by treating the laser as a two-wavelength light source: The weaker of the two dominating modes is firstly chosen and then compared with the strongest component among the rest sidebands. The obtained power difference in dB is R. This can be also be confirmed from Fig. 3(b-ii) where there is no observable peak corresponding to the second harmonic at the frequency of 24.9 GHz (=2×12.45 GHz).

As demonstrated in [45], the delay time plays a critical role on the stability of the RF signal formation in a mutually coupled semiconductor lasers system. We can find that for low values of delay time, undesired states for microwave signal generation such as period-two (P2), quasi-period (QP) and chaotic oscillation can be greatly suppressed in a large current-tuning range. In our scheme, the back-to-back mutually coupled structure can guarantee that there is no time delay between the F-DFB and B-DFB. Thus, our monolithically integrated laser can output P1 oscillation in a very large region. In our experiment, the F-DFB is biased at 60 mA, while the current of the R-DFB ($I_{R\text{-}DFB}$) can be tuned from 40 to 100 mA. Our results show that once the bias-current of the R-DFB is above 42.5 mA, our laser always keeps in the P1 state.

III. Discussions

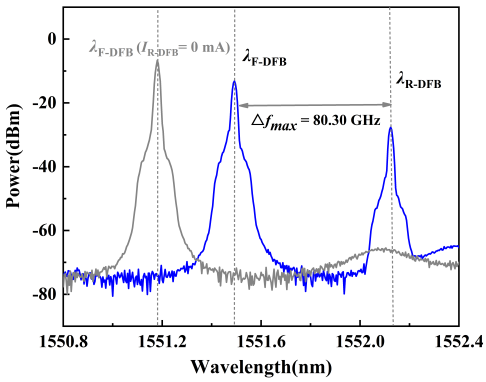

Fig. 4. Blue line: measured optical spectrum of the MITL with the maximal detuning frequency, where the current of $I_{F\text{-}DFB}$ is biased at 60 mA and the current of $I_{R\text{-}DFB}$ is biased at its available maximum current of 100 mA. Gray line: measured optical spectrum of the free-running F-DFB, which is the same as that in Fig. 2 when $I_{F\text{-}DFB}$ = 60 mA and $I_{R\text{-}DFB}$=0 mA, respectively.

Firstly, we discuss the physical limit of the obtainable photonic microwave signal using our laser. As the current $I_{R\text{-}DFB}$ increases in the experiment, the lasing wavelength of the R-DFB moves toward the longer wavelength obviously, while the wavelength of F-DFB changes slightly. From this point of view, the maximal detuning frequency can be expected when $I_{R\text{-}DFB}$ is set to be its available maximum current of 100 mA. Fig. 4 shows the associated optical spectrum. The optical spectrum of the laser in P1 oscillation has two significant characteristics different with that of a normal DFB laser: (i) the wavelength of the DFB laser in P1 oscillation has a red shift than that of the free-running normal DFB laser [45]; (ii) The linewidth of the DFB laser in P1 oscillation is wider than that of the free-running normal DFB laser [21]. To make this point clear, we insert the measured optical spectrum of the free-running F-DFB (grey line) in Fig. 4 in contrast with the optical spectrum of the MITL with the maximal detuning frequency (blue line). As can be seen, the wavelength of the F-DFB under injection indeed red-shifts from the free-running wavelength of 1551.179 nm to 1551.490 nm. Moreover, the linewidth of the F-DFB under injection is slightly broaden compared with that in free-running. This means that our MITL works at P1 state and thus can be viewed as the evidence of the microwave generation. From Fig. 4 (blue line), we can confirm the detuning frequency comes up to a high value of 80.30 GHz. That means that using the present MITL can output photonic microwave signal with the maximum frequency of about 80 GHz in principle.

Furthermore, the relationship between the after-injection detuning frequency Δf with the bias current of R-DFB is investigated. Here, we point that the result above 50 GHz is calculated according to the measured detuning frequency between the two dominant modes, rather than the actual RF measurement. As illustrated in Fig. 5, solid dots are experimental data and the red dashed line is a fitted line. After calculation, the linearity r^2 between the detuning frequency Δf and the bias current $I_{R\text{-}DFB}$ is as high as 0.99 [Note, r^2=1 for perfect linearity]. In other words, the MITL can generate continuously and linearly tuning microwave signals over a very large range. Such a high linearity

can be explained as follows. The dynamical behaviors in mutually coupled lasers (MCLs) are mainly dependent on the detuning frequency, coupling strength and coupling delay [41], [42], [45]. Because of the back-to-back structure, there is no coupling delay in our MITL. So, the associated influence caused by coupling delay variation can be discounted. On the other hand, MCLs without coupling delay usually can realize the P1 oscillation in a large parameter region [45]. When MCLs operate at a significant detuning frequency (corresponding to a relatively strong injection), the system will be dominated by the detuning frequency and always exhibits P1 oscillation [46]. Considering that the bias current of the F-DFB is fixed, the detuning frequency is mainly determined by the red-shift induced by the cavity resonance shift due to the optical injection from the R-DFB [41], [42]. This cavity resonance shift increases almost linearly with the increase of the coupling strength [42]. The coupling strength is linear with the bias current of the R-DFB in our experiment, so the generated microwave signals can be linearly tuned in a very large range.

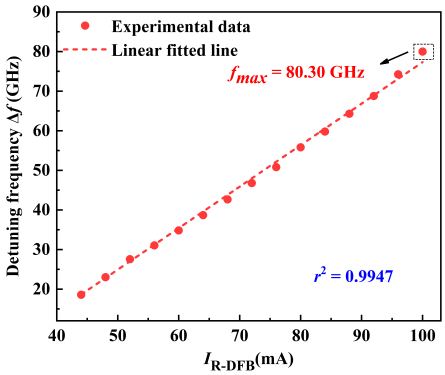

Fig. 5. The relationship between the optical detuning frequency Δf with the current of R-DFB. The current of $I_{F\text{-}DFB}$ is fixed at 60 mA, and the current of $I_{R\text{-}DFB}$ is adjusted from 44 to 100 mA with a 4-mA step.

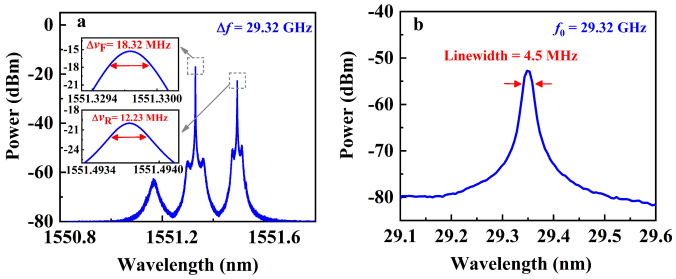

Fig. 6. (a) Measured optical spectrum and (b) RF spectrum when generated microwave frequency f_0 is about 29.32 GHz.

Figure 6 shows the measured optical spectrum and the associated RF spectrum when the generated microwave signal is about 29.32 GHz. Note, the optical spectrum in Fig. 6(a) is measured using an advanced optical spectrum analyzer (APEX AP2041B) with an ultrahigh resolution of 0.04 pm. After calculation, it can be determined that the linewidth $\Delta\nu_F$ and $\Delta\nu_R$ are 18.32 MHz and 12.23 MHz, respectively. From Fig. 6(b), it can be observed that the generated microwave signal has a much narrower linewidth of 4.5 MHz, which is less than the sum of the optical linewidths. This indicates that our horizontal integration of the DFB lasers with two optical modes sharing the same optical cavity can make their phase be partially correlated, and thus can increase the purity of the generated microwave signal.

Figure 7 shows the measured frequency variation of the generated microwave signal within 100 minutes. In the measurement, we recorded the center frequency of generated microwave signal every 5 minutes. It can be seen clearly from Fig. 7 that the frequency varies within a range of ±2.15 MHz, which is a relatively normal level for P1-based microwave generator. This long-term stability is expected to be significantly reduced from several MHz to KHz by further introducing external optical feedback [21, 23, 24, 28, 29, 31], optical injection [33], filtered feedback [34], or phase-locked loop [47]. This is the aim of our next work.

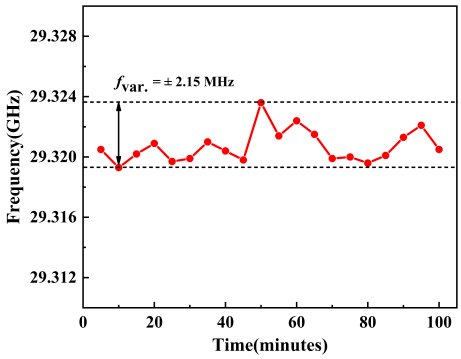

Fig. 7. Frequency stability of the microwave signal from MITL when the f_0 is 29.32 GHz. (Spectrum analyzer Setup: center frequency is set at 29.32 GHz, span is set at 100 MHz, RBW is set at 100 kHz).

We list some typical photonic integrated chips for photonic microwave generation in Table 1. In general, there are mainly two kinds of techniques that has been photonic integrated in a chip: optical heterodyne and P1 oscillation. From this table, one can see clearly that the generated microwave signal by optical heterodyne technique can reach up to the THz range by detecting two optical beams with different wavelengths. Typically, Dijk *et al.* realized millimeter-wave generation at up to 105 GHz based on heterodyning the optical tones from two integrated lasers [48]. Lo *et al.* proposed a monolithically integrated microwave frequency synthesizer where two tunable monochromatic lasers spectrally separated by 0-10.7 nm were realized [12]. Wei *et al.* demonstrated a widely tuning range of 1 GHz to 2.275 THz using feedback-cavities integrated two DBR lasers [13]. Kim et al. designed two monolithic dual-wavelength lasers with tuning ranges of 0.17- 0.79 THz [49] and 0.48 - 0.15 THz [50], respectively. However, it also must be pointed that the linewidths of the optical heterodyne microwave generator are very large (tens of MHz) corresponding to high phase noise levels. By contrast, the P1-based technique can greatly induce the phase noise of the generated microwave signal. Quantitatively, it can be confirmed from Table 1 that no matter the optical feedback laser [51] or optical injection laser [33], the linewidths of their generated microwave signals is at the level of few MHz. In particularly, we must emphasize that, different with the structure with three sections in [33], the elimination of phase section enables that our scheme not only has a simple structure and achieves a broad tuning range of tens or even hundreds of GHz. In sum, our scheme processes both two merits of the

TABLE 1. COMPARISON OF PHOTONIC INTEGRATED LASER CHIPS FOR MICROWAVE GENERATION.

Realization principle	Chip structure	Tuning range	Optical linewidth	RF Linewidth (before narrowing)	Ref.
Optical heterodyne	Two DFBs, an MMI coupler, eight SOAs, an electro-optical modulator and a UTC PD.	5 to 110 GHz	/	/	[48]
	Two wavelength tunable DFB lasers, an MMI coupler and a PIN-PD.	0-10.7 nm	20 to 40 MHz	90 MHz	[12]
	Two DBR-LDs, a feedback cavity, and two MMIs.	1 GHz-2.275 THz	/	11 MHz	[13]
	Two DFB sections, a phase section.	0.17 to 0.49 THz	/	/	[49]
	A phase-shifted DFB section, a phase section, a DBR section.	0.48 to 1.5 THz	5.6 MHz	/	[50]
P1 oscillation	A DFB section, a phase section and an amplifier section.	30 to 38 GHz	/	3.7 MHz	[51]
	Two DFB sections and a phase section	15 to 30 GHz	/	1.9 to 3.2 MHz	[33]
	Two DFB sections	12 to 80 GHz	Below 20 MHz	4.5 MHz	Our scheme

broad tuning range and low phase noise at the same time and thus has the potential to be widely used for microwave generation in practice.

IV. Conclusion

In summary, we have proposed and demonstrated experimentally a MITL for photonic microwave generation. Based on P1 oscillation in the back-to-back coupled structure, this MITL can output wideband and frequency-tunable photonic microwave signals with a large operation frequency range from 12 to 80 GHz. Moreover, the frequency of generated microwave signals can be tuned by simply adjusting the bias current with a high linearity of 0.99. Considering its chip-scale size, simple structure and good performance, we believe that this MITL can be a promising candidate as a photonic microwave generator for many applications such as wireless communications and microwave photonic radars.

References

[1] S. Koenig, D. Lopez-Diaz, J. Antes, F. Boes, R. Henneberger, A. Leuther, A. Tessmann, R. Schmogrow, D. Hillerkuss, R. Palmer, T. Zwick, C. Koos, W. Freude, O. Ambacher, J. Leuthold, and I. Kallfass, "Wireless sub-THz communication system with high data rate," *Nat. Photonics*, vol. 7, no. 12, pp. 977–981, Jul. 2013, doi: 10.1038/nphoton.2013.275.

[2] S. E. Alavi, M. R. K. Soltanian, I. S. Amiri, M. Khalily, A. S. M. Supa'at, H. Ahmad, "Towards 5G: a photonic based millimeter wave signal generation for applying in 5G access fronthaul," *Sci Rep*, vol. 6, Jan. 2016, Art. no. 19891, doi: 10.1038/srep19891.

[3] E. A. Kittlaus, D. Eliyahu, S. Ganji, S. Williams, A. B. Matsko, K. B. Cooper, S. Forouhar, "A low-noise photonic heterodyne synthesizer and its application to millimeter-wave radar," *Nat. Commun.*, vol. 12, no. 1, Jul. 2021. Art. no. 4397, doi: 10.1038/s41467-021-24637-0.

[4] X. Q. Qi, J. M. Liu, "Photonic microwave applications of the dynamics of semiconductor lasers," *IEEE J. Sel. Top. Quantum Electron.*, vol. 17, no. 5, pp. 1198-1211, Oct. 2011, doi: 10.1109/JSTQE.2011.2121055.

[5] S. K. Hwang, S. C. Chan, S. C. Hsieh, C. Y. Li, "Photonic microwave generation and transmission using direct modulation of stable injection-locked semiconductor lasers," *Opt. Commun.*, vol. 284, no. 14, pp. 3581-3589, Jul. 2011, doi: 10.1016/j.optcom.2011.03.066.

[6] O. Kjebon, R. Schatz, S. Lourdudoss, S. Nilsson, B. Stålnacke, L. Bäckbom, "30 GHz direct modulation bandwidth in detuned loaded InGaAsP DBR lasers at 1.55 μm wavelength," *Electron. Lett.*, vol. 33, no. 6, pp. 488-489, Mar. 1997, doi: 10.1049/el:19970335.

[7] G. Qi, J. Yao, J. Seregelyi, S. Paquet, C. Bélisle, "Generation and distribution of a wide-band continuously tunable millimeter-wave signal with an optical external modulation technique," *IEEE Trans. Microw. Theory Tech.*, vol. 53, no. 10, pp. 3090-3097, Oct. 2005, doi: 10.1109/TMTT.2005.855123.

[8] P. T. Shih, J. Chen, C. T. Lin, W. J. Jiang, H. S. Huang, P. C. Peng, S. Chi, "Optical millimeter-wave signal generation via frequency 12-Tupling," *J. Lightwave Technol.*, vol. 28, no. 1, pp. 71-78, Nov. 2010, doi: 10.1109/JLT.2009.2035452.

[9] X. S. Yao, L. Maleki, "Optoelectronic oscillator for photonic systems," *IEEE J. Quantum Electron.*, vol. 32, no. 7, pp. 1141-1149, Jul. 1996, doi: 10.1109/3.517013.

[10] S. Pan, J. Yao, "Wideband and frequency-tunable microwave generation using an optoelectronic oscillator incorporating a Fabry-Perot laser diode with external optical injection," *Opt. Lett.*, vol. 35, no. 11, pp. 1911-1913, Jun. 2010, doi: 10.1364/OL.35.001911.

[11] G. Carpintero, K. Balakier, Z. Yang, R. C. Guzmán, A. Corradi, A. Jimenez, G. Kervella, M. J. Fice, M. Lamponi, M. Chitoui, F. van Dijk, C. C. Renaud, A. Wonfor, E. A. J. M. Bente, R. V. Penty, I. H. White, A. J. Seeds, "Microwave photonic integrated circuits for millimeter-wave wireless communications," *J. Lightwave Technol.*, vol. 32, no. 20, pp. 3495-3501, Oct. 2014, doi: 10.1109/JLT.2014.2321573.

[12] M. C. Lo, A. Zarzuelo, R. Guzmán, G. Carpintero, "Monolithically integrated microwave frequency synthesizer on InP generic foundry platform," *J. Lightwave Technol.*, vol. 36, no. 19, pp. 4626–4632, Oct. 2018, doi: 10.1109/JLT.2018.2836298.

[13] W. Wei, P. Lin, L. Nie, S. Ke, X. Zeng, "A monolithically integrated

photonic microwave generator," *Laser Phys. Lett.*, vol. 15, no. 1, Jan. 2018, Art. no. 016201, doi: 10.1088/1612-202X/aa9319.

[14] J. Sun, Y. Dai, X. Chen, Y. Zhang, S. Xie, "Stable dual-wavelength DFB fiber laser with separate resonant cavities and its application in tunable microwave generation" IEEE Photon. Technol. Lett., vol. 18, no.24, pp. 2587-2589, Dec. 2006, doi: 10.1109/LPT.2006.887336.

[15] Y. H. Lo, Y. C. Wu, S. C. Hsu, Y. C. Hwang, B. C. Chen, and C. C. Lin, "Tunable microwave generation of a monolithic dual-wavelength distributed feedback laser," *Opt. Express*, vol. 22, no. 11, pp. 13125-13137, Jun. 2014, doi: 10.1364/OE.22.013125.

[16] Y. Zhou1, Z. Lu, L. Li, Y. Zhang, J. Zheng, Y. Du, L. Zou, Y. Shi, X. Zhang, Y. Chen and X. Chen1, "Tunable microwave generation utilizing monolithic integrated two-section DFB laser," *Laser Phys.*, vol. 29, no. 4, pp. 046201, Feb. 2019, doi: 10.1088/1555-6611/ab0367.

[17] G. Chen, D. Huang, X. Zhang, H. Cao, "Photonic generation of a microwave signal by incorporating a delay interferometer and a saturable absorber," *Opt. Lett.*, vol. 33, no.6, pp.554-556, Mar. 2008, doi: 10.1364/OL.33.000554.

[18] S. C. Chan, S. K. Hwang, J. M. Liu, "Period-one oscillation for photonic microwave transmission using an optically injected semiconductor laser," *Opt. Express*, vol. 15, no. 22, pp. 14921-14935, Oct. 2007, doi: 10.1364/OE.15.014921.

[19] J. P. Zhuang, S. C. Chan, "Tunable photonic microwave generation using optically injected semiconductor laser dynamics with optical feedback stabilization," *Opt. Lett.*, vol. 38, no. 3, pp. 344-346, Feb. 2013, doi: 10.1364/OL.38.000344.

[20] K. H. Lo, S. K. Hwang, S. Donati, "Optical feedback stabilization of photonic microwave generation using period-one nonlinear dynamics of semiconductor lasers," *Opt. Express*, vol. 22, no. 15, pp. 18648-18661, Jul. 2014, doi: 10.1364/OE.22.018648.

[21] L. C. Lin, S. H. Liu, F. Y. Lin, "Stability of period-one (P1) oscillations generated by semiconductor lasers subject to optical injection or optical feedback," *Opt. Express*, vol. 25, no. 21, pp. 25523-25532, Oct. 2017 doi: 10.1364/OE.25.025523.

[22] L. Fan, G. Xia, J. Chen, X. Tang, Q. Liang and Z. Wu, "High-purity 60GHz band millimeter-wave generation based on optically injected semiconductor laser under subharmonic microwave modulation," *Opt. Express*, vol. 24, no. 16, pp. 18252-018264, Aug. 2016, doi: 10.1364/OE.24.018264.

[23] S. Ji, Y. Hong, P. S. Spencer, J. Benedikt and I. Davies, "Broad tunable photonic microwave generation based on period-one dynamics of optical injection vertical-cavity surface-emitting lasers," *Opt. Express*, vol. 25, no. 17, pp. 19863-19871, Aug. 2017, doi: 10.1364/OE.25.019863.

[24] C. Xue, D. Chang, Y. Fan, S. Ji, Z. Zhang, H. Lin, P. S. Spencer and Y. Hong, "Characteristics of microwave photonic signal generation using vertical-cavity surface-emitting lasers with optical injection and feedback," *J. Opt. Soc. Am. B.*, vol. 37, no. 5, pp. 1394-1400, May. 2020, doi: 10.1364/JOSAB.389890.

[25] Y. Huang, P. Zhou and N. Li, "Broad tunable photonic microwave generation in an optically pumped spin-VCSEL with optical feedback stabilization," *Opt. Lett.*, vol. 16, no. 13, pp. 3147-3150, Jul. 2021, doi: 10.1364/OL.431184.

[26] M. Almulla and J. M. Liu, "Linewidth characteristics of period-one dynamics induced by optically injected semiconductor lasers," *Opt. Express*, vol. 28, no. 10, pp. 14677-14693, May. 2020, doi: 10.1364/OE.391854.

[27] Z. F. Jiang, Z. M. Wu, W. Y. Yang, C. X. Hu, Y. H. Jin, Z. Z. Xiao and G. Q. Xia, "Numerical investigation on photonic microwave generation by a sole excited-state emitting quantum dot laser with optical injection and optical feedback," *Chin. Phys. B*, vol. 30, no. 5, May. 2021, Art. no. 050504, doi: 10.1088/1674-1056/abd2a8.

[28] L. Fan, Z. M. Wu, T. Deng, J. G. Wu, X. Tang, J. J. Chen, S. Mao and G. Q. Xia, "Subharmonic Microwave Modulation Stabilization of Tunable Photonic Microwave Generated by Period-One Nonlinear Dynamics of an Optically Injected Semiconductor Laser," *J. Lightwave Technol.*, vol. 32, no. 23, pp. 4058-4064, Dec. 2014, doi: 10.1109/JLT.2014.2362528.

[29] A. Quirce and A. Valle, "High-frequency microwave signal generation using multi-transverse mode VCSELs subject to two-frequency optical injection," *Opt. Express*, vol. 20, no. 12, pp. 13390-13401, Jun. 2012, doi: 10.1364/OE.20.013390.

[30] C. Xue, S. Ji, A. Wang, N. Jiang, K. Qiu and Y. Hong, "Narrow-linewidth single-frequency photonic microwave generation in optically injected semiconductor lasers with filtered optical feedback," *Opt. Lett.*, vol. 43, no. 17, pp. 4184-4187, Sep. 2018, doi: 10.1364/OL.43.004184.

[31] X. Zou, F. Zou, Z, Cao, B. Lu, X, Yan, G, Yu, X. Deng, B, Luo, L. Yan, W. Pan, J. Yao, A. M. J. Koonen, "A multifunctional photonic integrated circuit for diverse microwave signal generation, transmission, and processing," *Laser Photon. Rev.*, vol. 13, no. 6, Jun. 2019, Art. no. 1800240, doi: 10.1002/lpor.201800240.

[32] H. Qi, G. Chen, D. Lu, L. Zhao, "A Monolithically Integrated Laser-Photodetector Chip for On-Chip Photonic and Microwave Signal Generation," *Photonics*, vol. 6, no. 4, Dec. 2019, Art. no. 102, doi: 10.3390/photonics6040102.

[33] J. Li, T. Pu, J. Zheng, Y. Zhang, Y. Shi, H. Zhu, Y. Li, X. Zhang, G. Zhao, Y. Zhou, X. Chen, "Photonic generation of linearly chirped microwave waveforms using a monolithic integrated three-section laser," *Opt. Express*, vol. 26, no. 8, pp. 9676-9685, Apr. 2018, doi: 10.1364/OE.26.009676.

[34] D. Lin, C. Sun, B. Xiong, Y. Luo, "Nonlinear dynamics in integrated coupled DFB lasers with ultra-short delay," *Opt. Express*, vol. 22, no. 5, pp. 5614-5622, Mar. 2014, doi: 10.1364/OE.22.005614.

[35] J. Li, J. L. Zheng, T. Pu, X. Zhang, "Numerical investigation on the nonlinear dynamics of the monolithically integrated mutual injected semiconductor laser with short-coupled regime," in *Proc. IEEE Int. Conf. WCSP*, Nanjing, China, Oct. 21-23, 2020.

[36] U. Feiste, D. J. As, and A. Ehrhardt, "18 GHz all-optical frequency locking and clock recovery using a self-pulsating two-section DFB-laser," *IEEE Photon. Technol. Lett.*, vol. 6, no. 1, pp. 106-108, Jan. 1994, doi: 10.1109/68.265905.

[37] H. J. Wuensche, U. Bandelow, H. Wenzel, and D. D. Marcenac, "Self pulsations by mode degeneracy in two-section DFB lasers," *in Proc. SPIE*, vol. 2399, 1995, pp. 195–206.

[38] B. Sartorius, M. Mohrle, U. Feiste, "12-64 GHz continuous frequency tuning in self-pulsating 1.55-μm multiquantum-well DFB lasers," *IEEE J. Sel. Top Quantum. Electron.*, vol. 1, no. 2, pp. 535-538, Jun. 1995, doi: 10.1109/2944.401239.

[39] U. Bandelow, L. Recke, and B. Sandstede, "Frequency regions for forced locking of self-pulsating multi-section DFB lasers," *Opt. Commun.*, vol. 147, no. 1, pp. 212-218, Feb. 1998, doi: https://doi.org/10.1016/S0030-4018(97)00570-1.

[40] Y. Dai, X. Chen, "DFB semiconductor lasers based on reconstruction-equivalent-chirp technology," *Opt. Express*, vol. 15, no. 5, pp. 2348-2353, Mar. 2007, doi: 10.1364/OE.15.002348.

[41] M. Kuznetsov, "Theory of wavelength tuning in two-segment distributed feedback lasers," *IEEE J. Quantum Electron.*, vol. 24, no. 9, pp. 1837-1844, Sept. 1988, doi.: 10.1109/3.7125.

[42] A. Murakami, K. Kawashima, K. Atsuki, "Cavity resonance shift and bandwidth enhancement in semiconductor lasers with strong light injection," *IEEE J. Quantum Electron*., vol. 39, no. 10, pp. 1196-1204, Oct. 2003, doi.: 10.1109/JQE.2003.817583.

[43] S. C. Chen, "Analysis of an optically injected semiconductor laser for microwave generation," *IEEE J. Quantum. Electron.*, vol. 46, no. 3, pp. 421-428, Mar. 2010, doi: 10.1109/JQE.2009.2028900.

[44] S. K. Hwang, J. M. Liu, and J. K. White, "Characteristics of Period-One Oscillations in Semiconductor Lasers Subject to Optical Injection," *IEEE J. Sel. Top Quantum. Electron.*, vol. 10, no. 5, pp. 974-981, Sept. 2004, doi: 10.1109/JSTQE.2004.836017.

[45] L. Junges, J. A. C. Gallas, "Stability diagrams for continuous wide-range control of two mutually delay-coupled semiconductor lasers," *New J. Phys.*, vol. 17, May. 2015, Art. no. 053038, doi: 10.1088/1367-2630/17/5/053038.

[46] X. Li, W. Pan, B. Luo, D. Ma, "Nonlinear dynamics of two mutually injected external-cavity semiconductor lasers," *Semicond. Sci. Technol.*, vol. 21, no. 1, pp. 25–34, Jan. 2006, doi: 10.1088/0268-1242/21/1/005.

[47] T. B. Simpson, "Phase-locked microwave-frequency modulations in optically-injected laser diodes," *Opt. Commun.*, vol. 170, pp. 93–98, Oct. 1999, doi: 10.1016/S0030-4018(99)00442-3.

[48] F. V. Dijk, G. Kervella, M. Lamponi, M. Chtioui, F. Lelarge, E. Vinet, Y. Robert, M. J. Fice, C. C. Renaud, A. Jimenez, G. Carpintero "Integrated InP Heterodyne Millimeter Wave Transmitter," *IEEE Photon. Technol. Lett.*, vol. 26, no. 10, pp. 965-968, May. 15, 2014, doi: 10.1109/LPT.2014.2309353.

[49] N. Kim, J. Shin, E. Sim, C. W. Lee, D. S. Yee, M. Y. Jeon, Y. Jang, K. H. Park, "Monolithic dual-mode distributed feedback semiconductor laser for tunable continuous-wave terahertz generation," *Opt. Express*, vol. 17, no. 16, pp. 13851-13859, Aug. 2009, doi: 10.1364/OE.17.013851.

[50] N. Kim, S. P. Han, H. C. Ryu, H. Ko, J. W. Park, D. Lee, M. Y. Jeon, and K. H. Park, "Distributed feedback laser diode integrated with distributed

Bragg reflector for continuous-wave terahertz generation," *Opt. Express,* vol. 20, no. 16, pp. 17496-17502, Jul. 2012, doi: 10.1364/OE.20.017496.

[51] B. Pan, D. Lu, Y. Sun, L. Yu, L. Zhang, L. Zhao, "Tunable optical microwave generation using self-injection locked monolithic dual-wavelength amplified feedback laser," *Opt. Lett.*, vol. 39, no. 22, pp. 6395-6398, Nov. 2014, doi: 10.1364/OL.39.006395.

Qiang Cai received the B.S. degree in optoelectronic information Science and Engineering from Taiyuan University of Science and Technology, Shanxi, China, in 2017. He is currently working toward the Ph.D. degree at the Key Laboratory of Advanced Transducers and Intelligent Control System (Ministry of Education of China), Taiyuan University of Technology, Shanxi, China.

His current research interests include nonlinear dynamics of semiconductor lasers.

Yunshan Zhang received the B.S. degree in science and technology of electronics from Shandong University, Jinan, Shandong, China, in 2002, and the Ph.D. degree in physical electronics from the Beijing Institute of Technology, Beijing, China, in 2011.

From 2013 to 2015, he was a Post-Doctoral Researcher with the College of Engineering and Applied Sciences, Nanjing University, Nanjing, Jiangsu, China, majoring in the design of DFB lasers and laser arrays. He is currently an Associate Professor with the Nanjing University of Posts and Telecommunications, Nanjing. His research interests include solid state lasers, DFB semiconductor lasers, fiber communication, and photonic integrated circuits.

Jilin Zheng received the B.S. and Ph.D. degrees in electromagnetic field and microwave technology from the PLA University of Science and Technology, Nanjing, China, in 2005 and 2010, respectively.

He is currently with the College of Communications Engineering, Army Engineering University of PLA, Nanjing, China. His research interests include microwave-photonics, DFB semiconductor lasers, fiber communication, and photonic integrated circuits. He is currently majoring in advanced DFB lasers and their applications.

Yamei Zhang (Member, IEEE) received the B.S. and Ph.D. degrees from the Nanjing University of Aeronautics and Astronautics, Nanjing, China, in 2012 and 2018, respectively.

She is currently with the Key Laboratory of Radar Imaging and Microwave Photonics and the Ministry of Education, Nanjing University of Aeronautics and Astronautics, Nanjing, China. Her research interests include microwave photonic signal generation and processing and ultra-fast microwave photonics.

Pu Li received the M.S. degree in physical electronics from Taiyuan University of Technology (TYUT), Shanxi, China, in 2011, and the Ph.D. degree in circuits and systems from the Key Laboratory of Advanced Transducers and Intelligent Control System (Ministry of Education of China), TYUT, in 2014.

In 2014, he joined TYUT as a lecturer. He was a Visiting Scholar with the School of Electronic Engineering, Bangor University, U.K., in 2017. Since 2018, he is a Professor the Key Laboratory of Advanced Transducers and Intelligent Control System (Ministry of Education of China), TYUT. His research interests include nonlinear dynamics of semiconductor lasers and its applications.

Prof. Li a Senior Member of the Chinese Optical Society and serves as a Reviewer for journals of the IEEE, OSA, and Elsevier organizations.

K. Alan Shore (SM'95) received the B.A. degree in mathematics from the University of Oxford, Oxford, U.K., and the Ph.D. degree from the University College, Cardiff, Wales, U.K.

He was a Lecturer with the University of Liverpool from1979 to 1983 and with the University of Bath, where he became a Senior Lecturer in 1986, a Reader in 1990, and a Professor in 1995. He was a Visiting Researcher with the Center for High Technology Materials, University of New Mexico, Albuquerque, USA, in 1987. In 1989, he was a Visiting Researcher with Huygens Laboratory, Leiden University, The Netherlands. From 1990 to 1991, he was with Teledanmark Research Laboratory and the MIDIT Center of the Technical University of Denmark, Lyngby. He was a Guest Researcher with the Electrotechnical Laboratory, Tsukuba, Japan, in 1991. In 1992, he was a Visiting Professor with the Department of Physics, University de les llles Balears, Palma-Majorca, Spain. He was a Visiting Lecturer with the Instituto de Fisica de Cantabria, Santander, Spain, from 1996 to 1998, and a Visiting Researcher with the Department of Physics, Macquarie University, Sydney, Australia, in 1996, 1998, 2000, 2002, 2005, and 2008. In 2001, he was a Visiting Researcher with the ATR Adaptive Communications Laboratories, Kyoto, Japan. From 2001 to 2008, he was the Director of Industrial and Commercial Optoelectronics, a Welsh Development Agency Center of Excellence. Since 1995, he has been the Head of the School of Informatics, College of Physical and Applied Sciences, Bangor University. He has authored or coauthored more than 1000 contributions to archival journals, books, and technical conferences. With Prof. D. Kane, he coedited the research monograph Unlocking Dynamical Diversity. His research work has been principally in the area of semiconductor optoelectronic device design and experimental characterization with particular emphasis on nonlinearities in laser diodes and semiconductor optical waveguides. His current research interests include nonlinear optics and its applications, and the design of nano-spin semiconductor lasers.

Dr. Shore has been a Program Member for several OSA conferences. He was a Co-Organizer of a Rank Prize Symposium on Nonlinear Dynamics in Lasers held at the lake district, U.K., in 2002. He co-founded and from 1987 to 2012 acted as the Organizer and Program Committee Chair for the International Conference on Semiconductor and Integrated Optoelectronics, which is held annually in Cardiff, Wales, U.K. He was the recipient of the Royal Society Travel Grant to visit universities and laboratories in Japan in 1988. From July to December 2010, he held a Japan Society for the Promotion of Science Invitation Fellowship in the Ultrafast Photonics Group, Graduate School of Materials Science, Nara Institute of Science and Technology, Nara, Japan. He is a Fellow of the Optical

Society of America, the Institute of Physics, and the Learned Society of Wales for which he has served as a Council Member (2012–2015; 2016–2023) and General Secretary (2017–2023).

Yuncai Wang received the B.S. degree in semiconductor physics from Nankai University, Tianjin, China, in 1986, and the M.S. and Ph.D. degrees in physics and optics from Xi'an Institute of Optics and Precision Mechanics, Chinese Academy of Sciences, Shaanxi, China, in 1994 and 1997, respectively.

In 1986, he joined TYUT as a Teaching Assistant. He was a Visiting Scholar in Technical University of Berlin, Berlin, Germany, from 2001–2002. He was a lecturer (1994–1998) and then an Assistant Professor (1998–2003) in the Department of Physics, TYUT. Since 2003, he has been a Professor in the College of Physics and Optoelectronics, TYUT. In 2019, he joined the Institute of Advanced Photonics Technology, Guangdong University of Technology. His current research interests include nonlinear dynamics of semiconductor lasers and its applications, chaos secure communication based on semiconductor lasers, millimeter wave signals generation and application.

Prof. Wang is a Fellow of the Chinese Instrument and Control Society, a Senior Member of the Chinese Optical Society and the Chinese Physical Society. He also serves as a Reviewer for journals of the IEEE, OSA, and Elsevier organizations.